Barhumi, Imad; Al-Tous, Hanan

Optimal Power Management in Energy Harvesting NOMA Enabled WSNs

Published in:
IEEE Internet of Things Journal

DOI:
10.1109/JIOT.2021.3114425

Published: 01/04/2022

Document Version
Peer-reviewed accepted author manuscript, also known as Final accepted manuscript or Post-print

Please cite the original version:
Barhumi, I., & Al-Tous, H. (2022). Optimal Power Management in Energy Harvesting NOMA Enabled WSNs. *IEEE Internet of Things Journal*, *9*(7), 4907-4916. https://doi.org/10.1109/JIOT.2021.3114425

Optimal Power Management in Energy Harvesting NOMA Enabled WSNs

Imad Barhumi* and Hanan Al-Tous**
*College of Engineering, UAE University, Al Ain, UAE
**Department of Communications and Networking, Aalto University, Espoo, Finland
Emails: imad.barhumi@uaeu.ac.ae, hanan.al-tous@aalto.fi

***Abstract*—Optimal resource allocation is crucial for successful deployment of energy harvesting wireless sensor networks (EH-WSN) such as Internet-of-Things (IoT) devices. Non-orthogonal multiple-access (NOMA) can significantly improve the network throughput compared to orthogonal multiple-access (OMA). This paper considers optimal power management and data scheduling in multi-hop EH-WSN using NOMA. The EH-WSN consists of M sensor nodes aiming to transmit their data to a sink node. Assuming network connectivity, the multi-hop EH-WSN is represented by a directed graph. The resource allocation problem is formulated to efficiently utilize the available harvested energy to send the available data to the sink node with minimum cost. The resource allocation problem given the system dynamics is non-convex due to the non-convex constraints. Assuming high signal-to-interference and noise ratio (SINR), the non-convex constraints are lower bounded by convex constraints. With the aid of variable transformation, the constrained non-convex problem is approximated with a convex problem. The convex problem is solved using finite horizon dynamic programming considering offline and online operations. The offline problem is formulated assuming non-causal information of the harvested energy and data arrival. Model predictive control (MPC) framework is used to obtain the solution of the online operation of the EH-WSN. A distributed MPC (DMPC) is proposed to overcome the computational complexity of solving the centralized MPC problem, assuming each sensor node is allowed to exchange information with its neighboring nodes. In the simulations, we use energy efficiency and average data transmitted to compare the performance of the EH-WSN using NOMA and OMA. Simulation results confirm that NOMA in multi-hop EH-WSN results in higher throughput compared to OMA.**

***Index Terms*—Wireless sensor network, IoT devices, energy harvesting, NOMA, OMA, resource allocation, model predictive control (MPC).**

I. INTRODUCTION

It is envisioned to have billions of Internet-of-Things (IoT) devices to be interconnected in the near future. The applications of these devices range from environmental monitoring, home-automation, healthcare, smart cities, irrigation in rural areas, and many more. Researchers expect that by the year 2030 there will be more than 50 Billion IoT devices [1], [2]. For full deployment of such autonomous networks requires tremendous cooperation among the wireless sensor nodes, where each sensor node assists in transmitting the data of neighboring nodes in addition to its own data. This may result in an increase in the energy demand of the sensor nodes, and therefore, in rural and inaccessible areas, it may not be possible to use standard battery powered nodes [3], [4].

Energy harvesting (EH) techniques have the potential to overcome the battery size constraints in wireless sensor networks (WSNs) and are key enablers for IoT devices. EH sensor nodes are equipped with circuits to harvest energy from the surroundings such as radio-frequency (RF), light, heat, vibration, etc. [5], [6].

Non-orthogonal multiple-access (NOMA) is a promising multiple access technique for future radio access that can significantly improve the system throughput. At the transmitter, superposition coding is used where the signals for various nodes is superposed and transmitted at the same channel (time and frequency). The receiver on the other hand, performs multi-user detection such as successive interference cancellation (SIC) [7]. Due to its effectiveness and improved connectivity, NOMA is a promising multiple-access technique for future IoT. NOMA provides high throughput/spectrum efficiency compared to OMA, which motivates its use for future IoT on the cost of higher computational complexity at the transmitter and receiver. Resource allocation such as power management and channel assignment are crucial to exploit the full benefits of NOMA system [8]. In NOMA enabled EH-WSNs, optimal power management is more challenging due to the system dynamics and the non-convexity of the optimization problem.

Model predictive control (MPC) or receding horizon control (RHC) is a framework that can be used to provide reliable energy-management policies when acceptable system model is available [9]. The aim of MPC is to determine an online optimal control vector that minimizes an objective function to reach a desired state for a given horizon assuming the knowledge of the system dynamics and the current state. MPC framework has been successfully applied to solve many online control problems such as cross-layer-design [10], robots formation [11], and power management of wireless sensor nodes [12].

In this paper, offline and online power management algorithms are proposed for NOMA EH-WSNs. The offline is formulated assuming non-causal state information, whereas the online approaches assume causal state information. The online algorithms are implemented based on MPC framework, where centralized and distributed MPC (DMPC) algorithms are considered. The objective function is formulated to drive the buffer-state to zero while regulating the used power. Each sensor node is assumed to be equipped with an energy harvesting circuit, a finite energy storage and a finite data buffer. The performance of the proposed online algorithms are compared with the offline algorithm in terms of the energy efficiency and average data transmitted across the network or received at the sink node. The network connectivity based on the network graph is utilized in the problem formulation. In the decentralized approach, the network is divided into sub-networks, each characterized by a sub-graph that is utilized in the formulation of the sub-problem. The solution is obtained for each sub-problem independently.

A. Related Work and Contributions

In this subsection, we survey the literature related to the solution approach and present the main contributions of the paper. In [10], MPC is considered for maximizing the wireless network utility to obtain an online optimal cross-layer network operation while accounting for the changes in the wireless channels. Each sensor node is assumed to have a battery of maximum transmission power, no energy harvesting capability is assumed. In [12], MPC based strategy is considered for power management of wireless sensor nodes. The network consists of multiple sensor nodes communicating with a sink node directly, no routing is considered. The objective function is formulated as a mixed integer quadratic programming problem aiming to achieve a target quality of service with a minimum number of active nodes. In [13], the authors propose power control and data transmission for OMA EH-WSNs using differential game theory. The open-loop Nash equilibrium is obtained based on receding horizon control. Similarly, optimal power control and data scheduling are devised based on centralized MPC algorithm for OMA EH-WSNs in [14].

In [15], the authors studied energy efficient resource allocation for machine-to-machine communication with energy harvesting. In there, the authors considered joint power control and time allocation assuming both NOMA and time-division multiple access (TDMA) schemes. The optimization problem was formulated to minimize the total power consumption via joint power control and time-allocation. The devices are assumed to be able to harvest energy from radio-frequency signals. In [16], the authors considered optimal energy-delay scheduling for EH-WSNs with interference channels. The non-convex resource allocation problem was solved using negatively correlated search, while in their earlier work [17], the non-convex optimization problem was transformed into a convex optimization problem by convex approximation. The optimization problem was formulated to minimize the total network delay by considering optimal data rates, power allocation and radio-frequency energy transfer. However, resource allocation problems in NOMA were thoroughly investigated under different setups. In most of these works, e.g., [8], [18], [19], the resource allocation problems were considered with no energy-harvesting assumptions or assuming either uplink or downlink scenarios.

The main contributions of this paper are summarized as follows:

- We consider optimal power management and data scheduling in NOMA enabled multi-hop EH-WSN, where the sensor nodes use superposition coding for transmission, and receiving nodes use SIC.
- The considered solution approaches are: offline, centralized online power management, and decentralized online power management.
- The online optimal power management is based on model predictive control. The offline is used as a benchmark for the performance of the online resource allocation approaches.
- The objective function is formulated to balance emptying the data buffers with minimum amount of power, taking into account the network connectivity using graph theory. The objective function is formulated as a quadratic function in the data state buffer and power control, assuming the system dynamics.
- The battery state is formulated assuming zero processing cost and non-zero processing cost. The non-zero processing cost is assumed to be an affine function of the amount of data transmitted and received.
- The formulated original problem is non-convex. Using high signal-to-interference and noise ratio (SINR), and variable transformation, the non-convex problem is approximated as a convex problem. The convex problem is solved using the interior point method.
- In the simulations, we evaluate the performance of the resource allocation problems using energy efficiency as well as the average amount of data transmitted across the networks or arrived at the sink node. Comparisons are made with frequency-division multiplexing OMA (FDM-OMA) scheme.
- To the best knowledge of the authors, this is the first time that MPC/RHC framework is applied for online operation of NOMA enabled multi-hop EH-WSNs.

The remainder of this paper is organized as follows. In Section II, the system model of the EH-WSNs is introduced. In Section III, the resource allocation problem, and the offline, MPC and DMPC algorithms are presented. Numerical results are presented and discussed in Section IV. Finally, conclusions are drawn in Section V.

II. System Model

The system under consideration is schematically shown in Figure 1. The WSN is assumed to consist of M energy-harvesting sensor nodes aiming to transmit their sensed and relayed data to a sink node using multi-hop communication. Each Sensor node is equipped with an energy harvesting circuit, a limited battery storage, and a limited buffer capacity. Sensor node S_i is allowed to communicate and exchange information with its next-hop set of neighbors denoted as $\mathcal{N}_i$. The channel gain $h^{(i,j)}$ of the (i, j) link between sensor node S_i and sensor node S_j is assumed to be constant throughout the transmission period. Transmission is arranged in time-slots of fixed duration of T sec, and a finite horizon of $K+1$ time-slots. In time-slot k, power $P_k^{(i,j)}$ is used to transmit $r_k^{(i,j)}$ bits over the link (i, j) using NOMA. Sensor node S_i uses multi-user superposition transmission (MUST) to transmit its data to its neighboring nodes. In this paper, power-domain NOMA

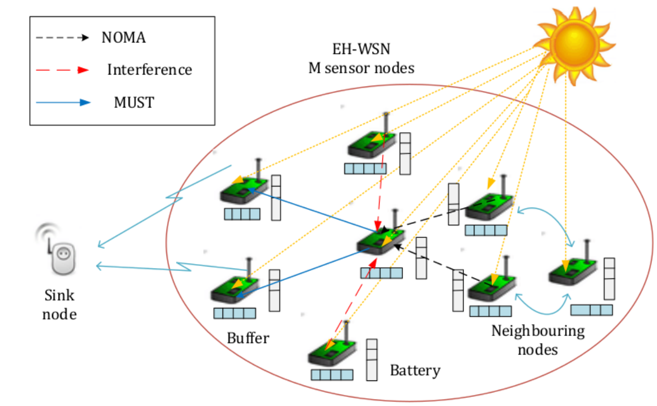

Fig. 1. System model: NOMA enabled EH-WSN.

multiplexing [7] is considered, where multiple sensors' data are superimposed in the power domain exploiting the channel gains differences.

The WSN is assumed to be static, and hence can be represented by a directed graph [20], where the communicating links are the edges and the sensor nodes are the vertices. Interference links from non-neighboring nodes are not captured by the graph. A directed graph $\mathcal{G} = (\mathcal{V}, \mathcal{E})$ consists of a set of vertices $\mathcal{V} = \{\nu_1, \dots, \nu_{M+1}\}$, indexed by the sensor nodes in the network and the sink node, and a set of directed edges $\mathcal{E} = \{(\nu_i, \nu_j) \in \mathcal{V} \times \mathcal{V}\}$, that contains ordered pairs of distinct vertices. A connected graph is assumed to enable data transmission in WSNs [21]. The WSN connectivity is assumed to be known at the deployment stage, and the modes of operations and users pairing are assumed to be static and known beforehand.

An edge-weighted graph $\mathcal{G} = (\mathcal{V}, \mathcal{E}, \boldsymbol{\omega})$ is a graph in which the edge (ν_i, ν_j) is assigned a weight $\omega_{ij} \geq 0$. The weight vector associated with the graph $\mathcal{G}$ is defined as $\boldsymbol{\omega}$. The Laplacian matrix $\boldsymbol{\mathcal{L}}$ is a positive definite matrix used to characterize an edge-weighted graph as [11]:

$$\boldsymbol{\mathcal{L}} = \boldsymbol{\mathcal{D}} \boldsymbol{\Omega} \boldsymbol{\mathcal{D}}^T, \tag{1}$$

where $\boldsymbol{\mathcal{D}}$ is a $(M+1) \times |\mathcal{E}|$ incidence matrix of the directed graph with entries $d_{ij} \in \{0, \pm 1\}$, and $\boldsymbol{\Omega} = \mathbf{diag}(\boldsymbol{\omega})$ is a $|\mathcal{E}| \times |\mathcal{E}|$ diagonal weight matrix. The (i,j)th entry of the incidence matrix is 1 if the source of edge j is node S_i, -1 if the tail of edge j is node S_i and 0 otherwise.

The sensor nodes are assumed to harvest energy at each time-slot without energy loss, and the harvested energy in time-slot k can be utilized in time-slot $k+1$. The state dynamics of the energy level of sensor node S_i for $i = 1, \dots, M+1$, evolves as:

$$E_{k+1}^{(i)} = E_k^{(i)} - T \sum_{j \in \mathcal{N}_i} P_k^{(i,j)} - \phi_k^{(i)} + H_k^{(i)}, \tag{2}$$

where $P_k^{(i,j)} \geq 0$ denotes the power level at time-slot k used to transmit $r_k^{(i,j)}$ bits from sensor node S_i to sensor node S_j, $\phi_k^{(i)}$ is the processing (circuitry) energy cost, and $H_k^{(i)}$ is the harvested energy of sensor node S_i during time-slot k. The stored energy overflow constraint of the battery of sensor node S_i is expressed as:

$$0 \leq E_k^{(i)} \leq E_{\max}^{(i)}. \tag{3}$$

Since the harvested energy needs to be stored in the battery before being used for transmission, the transmitted energy feasibility constraint is stated as:

$$T \sum_{j \in \mathcal{N}_i} P_k^{(i,j)} + \phi_k^{(i)} \leq E_k^{(i)}. \tag{4}$$

Similarly, the state dynamic of the data buffer of sensor node S_i can be written as:

$$C_{k+1}^{(i)} = C_k^{(i)} - \sum_{j \in \mathcal{N}_i} r_k^{(i,j)} + \sum_{j \in \mathcal{N}_i} r_k^{(j,i)} + d_k^{(i)}, \tag{5}$$

where $C_k^{(i)}$ is the amount of data contained in the buffer of sensor node S_i at time-slot k in bits, $d_k^{(i)}$ denotes the sensed data by the source node S_i and $r_k^{(j,i)}$ is the received data from sensor node S_j for $j \in \mathcal{N}_i$ at time-slot k. For the sink node S_{M+1}, the state dynamic of the data buffer evolves as:

$$C_{k+1}^{(M+1)} = C_k^{(M+1)} + \sum_{j \in \mathcal{N}_{M+1}} r_k^{(j,M+1)} + d_k^{(M+1)}. \tag{6}$$

The data buffer overflow constraint can be expressed as:

$$0 \leq C_k^{(i)} \leq C_{\max}^{(i)}. \tag{7}$$

The sink buffer is assumed to have a much larger capacity compared to the buffer of the source nodes, i.e., $C_{\max}^{(M+1)} \gg C_{\max}^{(i)}$ for $i = 1 \dots, M$. The transmitted data $r_k^{(i,j)}$ from sensor node S_i to a neighboring node S_j for $j \in \mathcal{N}_i$ at time-slot k are constrained by the channel capacity of the link as:

$$0 \leq r_k^{(i,j)} \leq TW \log_2 \left(1 + \Gamma_k^{(i,j)}\right), \tag{8}$$

where W is the channel bandwidth, and $\Gamma_k^{(i,j)}$ is the signal-to-interference and noise ratio (SINR) of the (i,j) link at time-slot k. Since the received data need to be stored in the buffer before being transmitted, data transmission feasibility constraint at sensor node S_i can be formulated as:

$$\sum_{j \in \mathcal{N}_i} r_k^{(i,j)} \leq C_k^{(i)}. \tag{9}$$

The SINR in (8) depends on the transmission reception mode of NOMA. In the following subsection, we will discuss these transmission modes, and give expression for the corresponding SINR.

A. NOMA Transmission Modes

In NOMA, the SINR depends on the position of the sensor node in the network which will define the type of interference based on the decoding scheme as follows. Let the normalized channel gain $\gamma^{(i,j)}$ be defined as: $\gamma^{(i,j)} = \frac{|h^{(i,j)}|^2}{\sigma^2}$ $\forall j \in \mathcal{N}_i$, with σ^2 is the noise power. Assume node S_i is communicating with next-hop neighboring nodes using MUST, and using the ordered channel gains as $\gamma^{(i,j_1)} > \gamma^{(i,j_2)} > \dots > \gamma^{(i,j_{N_i})}$, where $N_i = |\mathcal{N}_i|$, then the SINR $\Gamma^{(i,j_l)}$ for all $j_l \in \mathcal{N}_i$ is:

$$\Gamma_k^{(i,j_l)} = \frac{\gamma^{(i,j_l)} P_k^{(i,j_l)}}{\gamma^{(i,j_l)} \sum_{m=1}^{l-1} P_k^{(i,j_m)} + 1 + I_k^{(j_l)}}, \tag{10}$$

where $I_k^{(j_l)}$ accounts of other inter-interference at node j_l from neighboring nodes that are not within the same cluster of nodes but using the same resource block (RB).

Assume sensor node S_i is a next-hop node for multiple sensor nodes, and hence sensor S_i performs successive interference cancellation (SIC). Assume the channel gains are ordered as: $\gamma^{(j_1,i)} > \gamma^{(j_2,i)} > \ldots > \gamma^{(j_{M_i},i)}$, hence the SINR of the links connected to node S_i can be written as:

$$\Gamma_k^{(j_l,i)} = \frac{\gamma^{(j_l,i)} P_k^{(j_l,i)}}{\sum_{m=l+1}^{M_i} \gamma^{(j_m,i)} P_k^{(j_m,i)} + 1 + I_k^{(i)}}, \quad (11)$$

where M_i is the number of nodes communicating with node S_i simultaneously as a next-hop.

Assuming non-zero processing cost at a sensor node S_i, the processing cost is greatly affected by these transmission modes. Hence, taking into consideration these transmission modes in NOMA, the processing cost can be broken into three parts: a fixed cost for circuitry operation, a transmission cost as a function of the transmission data rate, and a reception and/or decoding cost as a function of the decoded data streams' rates. The reception cost is of two parts: a SIC processing cost and a decoding cost. In OMA system, different models were considered for the processing cost as in [22]. In this paper, we consider the processing cost to be a linear function of the transmission data rate and the decoded data stream rates as follows. Assuming that sensor node S_i is communicating with next-hop neighboring nodes $S_j|_{j\in\mathcal{N}_i}$ using MUST, and performs SIC of received data streams from neighboring nodes S_{j_m} for $m = 1\ldots, M_i$ and possibly performs decoding of superimposed unintended data streams, the processing cost can be formulated as:

$$\phi_k^{(i)} = \epsilon_c + \epsilon_t \sum_{j\in\mathcal{N}_i} r_k^{(i,j)} + \epsilon_r \left(\sum_{m=1}^{M_i} \left(r_k^{(j_m,i)} + \sum_{l\in\mathcal{N}_{j_m,i}} r_k^{(j_m,l)} \right) \right) \quad (12)$$

where ϵ_c is the fixed circuitry processing cost in Joules, ϵ_t and ϵ_r are the transmission and reception processing cost coefficients in Joules/bit respectively, and $\mathcal{N}_{j_m,i}$ is the set of nodes such that $\gamma^{(j_m,i)} > \gamma^{(j_m,j)}, \forall j \in \mathcal{N}_{j_m}$.

III. Problem Formulation

Power allocation and data scheduling are critical for successful operation of EH-WSNs. In EH-WSNs, the resource allocation problem has many properties that differentiate it from the resource allocation in conventional WSNs. In EH-WSN, theoretically, the sensor node has access to unlimited source of energy, but this energy can only be utilized after being harvested and stored. The amount of harvested energy is not known in advance, and entails rapid spatial and temporal variations. Whereas, in conventional WSN, the sensor node has access to a limited and fixed source of energy, the spatial and temporal variations, and causality constraints are not applicable. To reap the full benefits of NOMA, optimal power allocation is more crucial than optimal power management in OMA systems. In NOMA, the users in the downlink scenario (MUST) are power multiplexed, therefore there will be no control on the additional interference in the system which will exhibit further degradation on the system throughput.

The main objective of the proposed resource allocation in EH-WSN is to maximize the life-time of the network by making a balance between utilizing the harvested energy and emptying the data buffers, which can be formulated using a quadratic-cost function as explained next.

In the following, we address resource allocation in EH-WSNs using three different scenarios as follows: First, the centralized offline resource allocation is addressed assuming non-causal knowledge of the harvested energy and sensed data. This scenario will serve as a benchmark for the performance of the proposed online approaches. Second, an online centralized resource allocation using MPC framework is addressed assuming causal knowledge of the harvested energy and sensed data. Third, an online distributed resource allocation is addressed using DMPC framework assuming causal knowledge of the harvested energy and sensed data as well as information exchange between neighboring nodes.

A. *Offline Resource Allocation Problem*

The offline resource allocation problem is formulated assuming that a central unit has access to the non-causal information of the energy and data arrivals of all sensor nodes. The central unit will solve for the optimal power allocation and data scheduling and disseminate the optimal solution to all sensor nodes.

To drive sensor nodes to the desired zero-state vector (empty buffers), the network error can be expressed based on graph connectivity as:

$$z_k = \sum_{(i,j)\in\mathcal{E}} w_{ij} \Big(\frac{C_k^{(i)}}{C_{\max}^{(i)}} - \frac{C_k^{(j)}}{C_{\max}^{(j)}} \Big)^2,$$

which can be written using matrix notation as:

$$z_k = \boldsymbol{c}_k^T \boldsymbol{Q} \boldsymbol{c}_k, \quad (13)$$

where $\boldsymbol{c}_k = [C_k^{(1)}, \ldots, C_k^{(M+1)}]^T$ is the buffer state vector of all sensor nodes at time-slot k, and $\boldsymbol{Q}$ is the buffer state weighting matrix defined based on the directed graph of the WSN as: $\boldsymbol{Q} = \boldsymbol{\Lambda}^{-1}\boldsymbol{\mathcal{D}}\boldsymbol{\Omega}\boldsymbol{\mathcal{D}}^T\boldsymbol{\Lambda}^{-1}$, with $\boldsymbol{\Lambda} = \mathbf{diag}\big([C_{\max}^{(1)}, \ldots, C_{\max}^{(M+1)}]\big)$ is a diagonal matrix to handle an agreement on the buffer state when sensor nodes have different maximum capacities. Assuming sensor nodes S_i and S_j forming an edge (link (i,j)), and sensor node S_j is a next-hop for sensor node S_i, minimizing the difference of the normalized buffer states of the two nodes can be done by either balancing the amount of data stored in each buffer or by emptying the buffers. In dynamical systems, emptying the buffer will be generally the solution approach. In order to account for the minimum power used to empty the buffers, a regularization term based on the control vector is added. This will balance emptying the buffer and utilizing the harvested energy. Hence, we can formulate a quadratic objective function that consists of the two parts as follows:

$$\mathcal{U}(\boldsymbol{c}, \boldsymbol{p}) = \sum_{k=1}^{K} \boldsymbol{c}_k^T \boldsymbol{Q}_k \boldsymbol{c}_k + \sum_{k=0}^{K-1} \sum_{i=1}^{M} \boldsymbol{p}_k^{(i)T} \boldsymbol{R}_k^{(i)} \boldsymbol{p}_k^{(i)}, \quad (14)$$

where $\boldsymbol{c}=[\boldsymbol{c}_0^T,\ldots,\boldsymbol{c}_K^T]^T$ is the buffer state vector of all sensor nodes, and $\boldsymbol{p}=[\boldsymbol{p}_0^{(1)T},\ldots,\boldsymbol{p}_{K-1}^{(1)T},\ldots,\boldsymbol{p}_0^{(M)T},\ldots,\boldsymbol{p}_{K-1}^{(M)T}]^T$ is the power control vector of all sensor nodes with $\boldsymbol{p}_k^{(i)}=[P_k^{(i,j)}|_{\forall j\in\mathcal{N}_i}]^T$ is the power control vector of sensor node S_i at time-slot k. The weighting matrices $\boldsymbol{Q}_k$ and $\boldsymbol{R}_k^{(i)}$ are chosen as positive semi-definite matrices, with $\boldsymbol{Q}_k=\alpha_k\boldsymbol{Q}$, where α_k is some regularization factor. Without loss of generality, the regularization coefficient may be chosen to be constant. Large values of $\boldsymbol{Q}_k$ in comparison to $\boldsymbol{R}_k^{(i)}$ drives the buffer state vector to the origin quickly at the expense of large control (power) action. Penalizing the control action of sensor node S_i through large values of $\boldsymbol{R}_k^{(i)}$ relative to $\boldsymbol{Q}_k$ is the way to reduce the control action and slow down the rate at which the buffer state vector approaches the origin.

The offline resource allocation problem can then be formulated taking into consideration the limited battery capacity and data buffer size of each sensor node as:

$$\min_{\boldsymbol{r},\,\boldsymbol{p},\,\boldsymbol{c},\,\boldsymbol{e}} \mathcal{U}(\boldsymbol{c},\boldsymbol{p}), \tag{15a}$$

subject to:

$$\text{given } \boldsymbol{e}_0 \,\&\, \boldsymbol{c}_0, \tag{15b}$$

$$\text{(2)-(9)},\ \text{ for } k=0,\ldots,K-1,\ \&\, i=1,\ldots,M+1, \tag{15c}$$

where $\boldsymbol{r}$ is the transmitted data control vector defined as $\boldsymbol{r}=[\boldsymbol{r}_0^{(1)T},\ldots,\boldsymbol{r}_{K-1}^{(1)T},\ldots,\boldsymbol{r}_0^{(M)T},\ldots,\boldsymbol{r}_{K-1}^{(M)T}]^T$, with $\boldsymbol{r}_k^{(i)}=[r_k^{(i,j)}|_{\forall j\in\mathcal{N}_i}]$, and the battery state vector $\boldsymbol{e}$ is defined as $\boldsymbol{e}=[E_0^{(1)},\ldots,E_K^{(1)},\ldots,E_0^{(M)},\ldots,E_K^{(M)}]^T$, with the initial energy state vector defined as $\boldsymbol{e}_0=[E_0^{(1)},\ldots,E_0^{(M)}]^T$. Similarly, the initial data state vector is defined as $\boldsymbol{c}_0=[C_0^{(1)},\ldots,C_0^{(M+1)}]^T$.

Problem (15) is a non-convex optimization problem, since in NOMA the data transmitted (8) is not a convex function with respect to the power due to interference. It can be solved using a global nonlinear solver such as Solving Constraint Integer Programs (SCIP) [23] with unavoidable computational complexity. However, convex approximation can be used to overcome the computational complexity. In this sense, using the lower bound approximation of the data rate ($\log(x)\le\log(1+x)$), and introducing a new variable $q_k^{(i,j)}$ such that $P_k^{(i,j)}-2^{q_k^{(i,j)}}\le y_k^{(i,j)}$, with $y_k^{(i,j)}\ge 0$ will result in a convex problem. Direct transformation of the power control $P_k^{(i,j)}=2^{q_k^{(i,j)}}$, is sufficient to transform the rate lower bound to a convex function, but the linear equality constraints of the energy state becomes non-convex. Hence, the variable $y_k^{(i,j)}$ is introduced in the optimization problem as a penalty term in the objective function as $\|\boldsymbol{y}\|_2^2$, where $\boldsymbol{y}=[\boldsymbol{y}_0^{(1)T},\ldots,\boldsymbol{y}_{K-1}^{(1)T},\ldots,\boldsymbol{y}_0^{(M)T},\ldots,\boldsymbol{y}_{K-1}^{(M)T}]^T$, with $\boldsymbol{y}_k^{(i)}=[y_k^{(i,j)}|_{\forall j\in\mathcal{N}_i}]^T$. Hence, the convex optimization problem can be stated as:

$$\min_{\boldsymbol{r},\,\boldsymbol{p},\,\boldsymbol{c},\,\boldsymbol{e}\,\boldsymbol{y},\,\boldsymbol{q}} \mathcal{U}(\boldsymbol{c},\boldsymbol{p})+\tau\|\boldsymbol{y}\|_2 \quad \text{subject to:} \tag{16a}$$

$$\text{given } \boldsymbol{e}_0 \,\&\, \boldsymbol{c}_0, \tag{16b}$$

$$\text{(2)-(7)},\ \&\ (9) \quad \text{for } i=1,\ldots,M,$$

$$\text{for } k=0,\ldots,K-1,\ \&\, i=1,\ldots,M+1, \tag{16c}$$

$$P_k^{(i,j)}-2^{q_k^{(i,j)}}\le y_k^{(i,j)}, \tag{16d}$$

$$y_k^{(i,j)}\ge 0,\quad \forall(i,j) \text{ links}, \tag{16e}$$

$$0\le r_k^{(i,j_l)}\le TW\Bigg(\log_2\gamma^{(i,j_l)}+q_k^{(i,j_l)}- \log_2\Bigg(\gamma^{(i,j_l)}\sum_{m=1}^{l-1}2^{q_k^{(i,j_m)}}+1+I_k^{(j_l)}\Bigg)\Bigg), \tag{16f}$$

$$0\le r_k^{(j_l,i)}\le TW\Bigg(\log_2\gamma^{(j_l,i)}+q_k^{(j_l,i)}- \log_2\Bigg(\sum_{m=l+1}^{M_i}\gamma^{(j_m,i)}2^{q_k^{(j_m,i)}}+1+I_k^{(i)}\Bigg)\Bigg), \tag{16g}$$

where $\tau>0$ is a regularization parameter. The constraint (16f) is relevant if sensor node S_i communicates with neighboring nodes using MUST, and constraint (16g) is relevant when sensor node S_i performs SIC. Since (16) is a convex optimization problem, it can be solved using different techniques such as the interior-point method [24]. The solution of (16) is usually used as a benchmark for the online MPC and DMPC solutions as explained next.

B. MPC Problem

MPC framework is used for the online resource allocation of EH-WSNs. MPC is explained as follows [9]: Consider a starting time-slot s and a horizon extending to N time-slots into the future, with $N\le K$. First, the central unit measures (or estimates) the buffer and battery states of all sensor nodes at time-slot s. Second, it computes the optimal control values of the power and transmitted data of all sensor nodes for all time slots $\{s,\ldots,s+N-1\}$ of the system by solving an optimization problem aiming to drive the buffer state of all sensor nodes to zero while using minimum energy. The control actions at time-slot s are then applied to the WSN. The starting time is shifted to time-slot $s+1$, and the same procedure is repeated again.

The objective (cost) function $\mathcal{U}_s(\boldsymbol{c},\boldsymbol{p})$ fitting the MPC framework of EH-WSNs starting at time-slot s and extending over a horizon of N time-slots is expressed as:

$$\mathcal{U}_s(\boldsymbol{c},\boldsymbol{p})=\sum_{k=s}^{s+N}\boldsymbol{c}_k^T\boldsymbol{Q}_k\boldsymbol{c}_k+\sum_{k=s}^{s+N-1}\sum_{i=1}^{M}\boldsymbol{p}_k^{(i)T}\boldsymbol{R}_k^{(i)}\boldsymbol{p}_k^{(i)}. \tag{17}$$

The EH-WSN control problem for one iteration of the MPC problem for $k=s,\ldots,s+N-1$ is expressed as:

$$\min_{\boldsymbol{r},\,\boldsymbol{p},\,\boldsymbol{c},\,\boldsymbol{e},\,\boldsymbol{y},\,\boldsymbol{q}} \mathcal{U}_s(\boldsymbol{c},\boldsymbol{p})+\tau\|\boldsymbol{y}\|_2, \quad \text{subject to:} \tag{18a}$$

$$\text{given } \boldsymbol{e}_s \,\&\, \boldsymbol{c}_s, \tag{18b}$$

$$\text{(3), (4), (7), (9), \& (16d)-(16g)}, \tag{18c}$$

$$E_{k+1}^{(i)}=E_k^{(i)}-T\sum_{j\in\mathcal{N}_i}P_k^{(i,j)}-\phi_k^{(i)}+\hat{H}_k^{(i)}, \tag{18d}$$

$$C_{k+1}^{(i)}=C_k^{(i)}-\sum_{j\in\mathcal{N}_i}r_k^{(i,j)}+\sum_{j\in\mathcal{N}_i}r_k^{(j,i)}+\hat{d}_k^{(i)}. \tag{18e}$$

At time slot $s\ge 0$, the measured (or estimated) battery and buffer states of all sensor nodes are given. Since the harvested energy and sensed data are unknown to the sensor nodes in (18d)-(18e), they are replaced by $\hat{H}_k^{(i)}$ and $\hat{d}_k^{(i)}$ respectively, which are either zero, or samples from their models if known. The measured state vectors of the battery and the buffer at

Algorithm 1 The MPC Algorithm.

1: **Given** the network parameters: T, W, σ^2, $h^{(i,j)}$, $C_{\max}^{(i)}$, $E_{\max}^{(i)}$, τ, $\boldsymbol{Q}_k$, $\boldsymbol{R}_k^{(i)}$, $i = 1, \ldots, M$, and N.
2: **At time-slot** s,
3: **Sensor node** S_i measures $E_s^{(i)}$ and $C_s^{(i)}$ and transmits
4: them to a central unit.
5: **The initial state vectors** $\boldsymbol{e}_s$ and $\boldsymbol{c}_s$ are constructed.
6: **Solve** (18).
7: **Each sensor node** S_i is informed of its control vectors
8: at time-slot s.
9: **Sensor node** S_i applies its control vector to the
10: network at time-slot s only.
11: **Recede** the horizon $s \leftarrow s + 1$,
12: **Go to** step 2

time-slot $s + 1$ take care of the harvested energy and the sensed data until time-slot s. The convex optimization problem (18) can be solved using different techniques such as the interior point-method. Many efficient algorithms for solving constrained-linear-quadratic MPC problems are developed in [25]. The MPC algorithm for the online operation of EH-WSNs is summarized in Algorithm 1.

C. DMPC Problem

In large-scale systems such as EH-WSNs, distributed resource allocation algorithms play an important role, in which the original large-size resource allocation problem is replaced by a number of smaller and easily tractable ones that work iteratively and cooperatively towards achieving the system objective. These smaller problems can be solved simultaneously with much reduced complexity compared to the online central solution. Several distributed resource allocation algorithms have been proposed in literature based on DMPC framework such as [26], [27]. DMPC algorithms are based on solving several MPC sub-problems at each time-slot, where each controller (sensor node or a set of nodes) locally solves an MPC sub-problem. In NOMA, multiple nodes will be involved in SIC and MUST, which means their decisions are coupled. Therefore, in the EH-WSN, a sub-graph of the main graph is formed of these decision nodes, and their next-hop nodes. For a sub-problem m, let $\mathcal{T}_m$ be the set of decision nodes, and $\mathcal{J}_m$ be the set of next-hop nodes, i.e. $\mathcal{J}_m = \bigcup_{i \in \mathcal{T}_m} \mathcal{N}_i$. A connected sub-graph is formed of the sensor nodes $\mathcal{V}_m = \mathcal{T}_m \cup \mathcal{J}_m$ and the corresponding connected edges.

In general, the local MPC sub-problem is of a much reduced computational complexity compared to the centralized MPC problem. In addition, DMPC framework reduces the communication overhead, since information exchange is limited to neighboring sensor nodes within the sub-graph. The local MPC sub-problems are designed to approximate the centralized MPC problem.

The resource allocation in EH-WSNs based on DMPC framework is explained as follows: consider a starting time-slot s and a horizon extending to N time-slots in the future. First, sensor node S_i for $i = 1, \ldots, M$ measures/estimates its battery and buffer states and exchanges information with neighboring sensor nodes. Second, a sub-graph is formed of decision nodes and their neighboring sensor nodes. The RHC problem is solved for this sub-graph and the optimal power values are communicated to the sensor nodes in the same sub-graph. The power control at the current time-slot is applied, then the horizon is shifted and the same procedure is repeated again at the next time-slot. The basics of DMPC for a constrained linear-quadratic dynamic system are reviewed in [26].

For an EH-WSN, similar to MPC and offline approaches, the proposed DMPC formulation aims to empty the buffers of all sensor nodes using minimum amount of energy in a cooperative fashion. The objective and the constraints of each MPC sub-problem are selected to capture the information structure of the network. The buffer state of each sensor node is affected by its control and the controls of its neighboring nodes. For a sub-graph m defined as the graph that involves the decision nodes in sub-problem m and their next-hop neighbors. The objective function $\mathcal{U}_s^{(m)}(\cdot)$ of sub-graph m for $m = 1, \ldots, G$, where G is the total number of sub-graphs in the EH-WSN, can be expressed as:

$$\begin{aligned}\mathcal{U}_s^{(m)}(\boldsymbol{c}^{(m)}, \boldsymbol{p}^{(m)}) = &\sum_{k=s}^{s+N} \boldsymbol{c}_k^{(m)T} \boldsymbol{Q}_k^{(m)} \boldsymbol{c}_k^{(m)} \\ &+ \sum_{k=s}^{s+N-1} \boldsymbol{p}_k^{(m)T} \boldsymbol{R}_k^{(m)} \boldsymbol{p}_k^{(m)},\end{aligned} \tag{19}$$

where $\boldsymbol{c}_k^{(m)} = [C_k^{(j)}|_{j \in \mathcal{V}_m}]^T$, then $\boldsymbol{c}^{(m)} = [\boldsymbol{c}_s^{(m)T}, \ldots, \boldsymbol{c}_{s+N}^{(m)T}]^T$, and $\boldsymbol{p}^{(m)} = [\boldsymbol{p}_s^{(m)T}, \ldots, \boldsymbol{p}_{s+N-1}^{(m)T}]^T$ with $\boldsymbol{p}_k^{(m)} = [p_k^{(j,l)}|_{j \in \mathcal{T}_m, l \in \mathcal{J}_m}]^T$. The buffer state vector weighting matrix $\boldsymbol{Q}_k^{(m)}$ is defined as $\boldsymbol{Q}_k^{(m)} = \boldsymbol{\Pi}^{(m)} \tilde{\boldsymbol{Q}}_k \boldsymbol{\Pi}^{(m)T}$, where $\boldsymbol{\Pi}^{(m)}$ is a selection matrix that selects the nodes within the sub-graph m, i.e., a sub-matrix of the identity matrix with the rows selected corresponding to the nodes within the sub-graph, $\tilde{\boldsymbol{Q}}_k$ is defined as $\boldsymbol{\Lambda}^{-1} \boldsymbol{D} \tilde{\boldsymbol{\Omega}}_k^{(m)} \boldsymbol{D}^T \boldsymbol{\Lambda}^{-1}$, where $\tilde{\boldsymbol{\Omega}}_k^{(m)}$ is the same as $\boldsymbol{\Omega}_k$ with the edges not in the sub-graph are assigned zero weight. The weight of the control action of sub-problem m at time-slot k is selected such that $\boldsymbol{R}_k^{(m)}$ is positive definite matrix.

The local MPC sub-problem m for $k = s, \cdots, s + N - 1$, is expressed as:

$$\min_{\boldsymbol{x}^{(m)}} \mathcal{U}_s^{(m)}(\boldsymbol{c}^{(m)}, \boldsymbol{p}^{(m)}) + \tau \|\boldsymbol{y}^{(m)}\|_2, \tag{20a}$$

subject to:

$$\text{given } \boldsymbol{c}_s^{(m)}, \boldsymbol{e}_s^{(m)}, \tag{20b}$$

$$(3), (4) \quad \forall i \in \mathcal{T}_m, \tag{20c}$$

$$(7), (9), (18d) \quad \forall i \in \mathcal{V}_m, \tag{20d}$$

$$C_{k+1}^{(i)} = C_k^{(i)} - \sum_{j \in \mathcal{N}_i} r_k^{(i,j)} + \hat{d}_k^{(i)}, \forall i \in \mathcal{T}_m, \tag{20e}$$

$$C_{k+1}^{(l)} = C_k^{(l)} + \sum_{i \in \mathcal{T}_m} r_k^{(i,l)} + \hat{d}_k^{(l)}, \quad \forall l \in \mathcal{J}_m, \tag{20f}$$

where $\boldsymbol{x}^{(m)} = [\boldsymbol{r}^{(m)T}, \boldsymbol{c}^{(m)T}, \boldsymbol{p}^{(m)T}, \boldsymbol{q}^{(m)T}, \boldsymbol{e}^{(m)T}, \boldsymbol{y}^{(m)T}]^T$ with $\boldsymbol{r}^{(m)}$, $\boldsymbol{q}^{(m)}$ and $\boldsymbol{y}^{(m)}$ are similarly defined as $\boldsymbol{p}^{(m)}$,

Algorithm 2 The DMPC Algorithm for Sub-problem m.

1: **Given** the network parameters: T, W, σ^2, τ, N, $\boldsymbol{Q}_k$, $\boldsymbol{R}_k^{(i)}$, $C_{\max}^{(i)}$, for $E_{\max}^{(i)}$, for $i \in \mathcal{V}_m$, $\gamma^{(l,j)}$, for $l \in \mathcal{T}_m$ and $j \in \mathcal{J}_m$.
2: **At time-slot** s,
3: **Exchange** of buffer and battery status of sub-graph m.
4: **Solve** (20).
5: **Communicate** the control vector to decision nodes of
6: sub-graph m.
7: **Decision nodes** take the action at time-slot s only.
8: **Recede** the horizon $s \leftarrow s+1$.
9: **Go to** step 2,

and $\boldsymbol{e}^{(m)}$ is defined as $\boldsymbol{c}^{(m)}$. Each sub-graph solves its local MPC problem (20) and only applies the control vector $[\boldsymbol{p}_s^{(m)T}, \ \boldsymbol{r}_s^{(m)T}]^T$. The buffer and battery states are then measured at sensor node S_i for $i = 1, \cdots, M$ and exchanged with neighboring nodes. The horizon is shifted one time-slot and the process is repeated again.

Note that constraints (20c) and (20d) approximate the original constraints in the centralized MPC problem, i.e., problem (20) takes into consideration that sensor node S_i knows its next-hop neighbors but does not know the neighbors of its neighbor. Similar to MPC, causal information of the harvested energy and sensed data at each sensor node is either set to zero, or randomly generated according to its model if known.

The DMPC algorithm is summarized in **Algorithm** 2. For the sub-problem m with sub-graph m, the sensor nodes within the sub-graph exchange their buffer and battery status. Given the current status of the sub-graph, (20) is solved locally for the sub-graph for a horizon of length N, the solution (control vector) is communicated to the decision nodes to take the action at time-slot s only. The horizon recedes to time-slot $s+1$, and the same algorithm is repeated. All sub-problems in the network are solved simultaneously.

IV. Simulation Results and Discussion

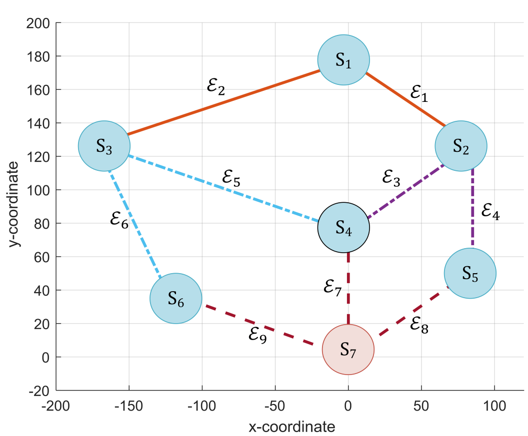

Fig. 2. The investigated scenario.

The EH-WSN under investigation consists of 7 sensor nodes as shown in Figure 2. Sensor nodes $\{S_1, \cdots, S_6\}$ are aiming to transmit their data to the sink node S_7. The channel gains are computed based on the distance between the sensor nodes as: $\gamma^{(i,j)} = \frac{d_{i,j}^{-\alpha}}{\sigma^2}$, where $d_{i,j}$ is the separating distance between sensor nodes S_i and sensor node S_j, $\alpha = 4$ is the propagation loss factor, and the noise power $\sigma^2 = -70$ dBm. The xy-coordinates (x_i, y_i) in meters of sensor node S_i for $i = 1, \cdots, 7$ are as shown in Figure 2. The incidence matrix $\boldsymbol{\mathcal{D}}$ of the EH-WSN in Figure 2 is given as:

$$\boldsymbol{\mathcal{D}} = \begin{bmatrix} 1 & 1 & 0 & 0 & 0 & 0 & 0 & 0 & 0 \\ -1 & 0 & 1 & 1 & 0 & 0 & 0 & 0 & 0 \\ 0 & -1 & 0 & 0 & 1 & 1 & 0 & 0 & 0 \\ 0 & 0 & -1 & 0 & -1 & 0 & 1 & 0 & 0 \\ 0 & 0 & 0 & -1 & 0 & 0 & 0 & 1 & 0 \\ 0 & 0 & 0 & 0 & 0 & -1 & 0 & 0 & 1 \\ 0 & 0 & 0 & 0 & 0 & 0 & -1 & -1 & -1 \end{bmatrix}.$$

In the considered WSN, sensor node S_1 performs superposition transmission, similarly sensor nodes S_2 and S_3. Sensor node S_2 decodes the information of sensor node S_3 before decoding its own information, whereas sensor node S_3 only decodes its information in the presence of interference from information transmitted to sensor node S_2. Sensor node S_4 performs partial interference cancellation from sensor node S_3, while considering information sent to sensor node S_5 as interference. The sink node S_7, performs SIC as ordered by the corresponding channel gains from sensor nodes S_4, S_5, and S_6. We assume time-independent weighting matrices, i.e., $\boldsymbol{Q}_k = \boldsymbol{Q}$ and $\boldsymbol{R}_k^{(i)} = 0.1\boldsymbol{I}_2$ for $i = 1, 2, 3$ and $R_k^{(i)} = 0.1$ for $i = 4, 5, 6$, where $\boldsymbol{I}_n$ is the $n \times n$ identity matrix. The energy processing cost for transmission equals the energy processing cost for reception and is identical at all sensor nodes, i.e., $\epsilon_t^{(i)} = \epsilon_r^{(i)} = \epsilon$, for $i = 1, \ldots, 7$. The regularization coefficient is chosen as $\tau = 0.01$

The harvested energy of sensor node S_i in time-slot k is modeled as a uniform random variable over $[0, H_{\max}]$, where $H_{\max} = 0.01$ Joules [28]. The data arrival at each sensor node is modeled as a Poisson random variable with arrival packet rate $\lambda = 1$ and packet size of 100 bits. Note that the harvested energy and sensed data models will not affect the solution approach. The solution at each step is affected only by the battery and data buffer status at each time-slot. The maximum buffer capacity is $C_{\max}^{(i)} = 10$ kbits for sensor nodes S_i for $i = 1, \cdots, 6$, and $C_{\max}^{(7)} = 10$ Mbits for the sink node. The maximum battery capacity is $E_{\max}^{(i)} = 1$ Joules for sensor nodes S_i for $i = 1, \cdots, 7$. Transmission is organized in time-slots with duration $T = 1$ ms, and the transmission bandwidth $W = 100$ kHz.

In this paper, first we compare the offline solution of the approximated convex problem (16) with that of the original non-convex optimization problem (15) using the global solver Solving Constraint Integer Programs (SCIP). Second, we compare the performance of the EH-WSN considering OMA and NOMA multiple access techniques. In this comparison, we consider the offline, MPC and DMPC solutions. In NOMA, the solutions are obtained by solving the approximated convex problems. The comparison is also considered under zero processing cost, and non-zero processing cost assumptions. In OMA, the non-zero processing is modeled as:

$$\phi_k^{(i)} = \epsilon_c + \epsilon_t \sum_{j \in \mathcal{N}_i} r_k^{(i,j)} + \epsilon_r \sum_{j \in \mathcal{N}_i} r_k^{(j,i)}. \tag{21}$$

The non-zero processing cost coefficients for OMA and NOMA are assumed as follows: $\epsilon_c = 1$ μJoules, and $\epsilon_r = \epsilon_t = 10$ μJoules/bit. OMA is implemented using frequency-division multiplexing (FDM), the optimization problem is formulated as a power-allocation problem and the frequency bands are equally divided. For fair comparison, the resource blocks in NOMA are assumed to be the same as those in OMA. In the simulation setup, three frequency resource blocks are assumed. The problems are solved using the CVX toolbox [29].

In the resource allocation problem formulations, we optimize over the transmitted data bits, and transmission power. Hence, in the following we use the energy efficiency as a metric for performance comparison measured at the sink node and/or across the network as a function of time-slot k. The energy efficiency in [bits/sec/Hz]/Joule at the sink node is defined as:

$$EE_k^{\text{sink}} = \frac{\sum_{l=0}^{k} \sum_{j \in \mathcal{N}_{M+1}} r_l^{(j,M+1)}}{TW \sum_{l=0}^{k} \sum_{i=1}^{M+1} \left(\phi_l^{(i)} + \tau \sum_{j \in \mathcal{N}_i} p_l^{(i,j)} \right)}, \tag{22}$$

and the global energy efficiency in [bits/sec/Hz]/Joule for the whole network is defined as:

$$EE_k^{\text{global}} = \frac{\sum_{l=0}^{k} \sum_{i=1}^{M} \sum_{j \in \mathcal{N}_i} r_l^{(i,j)}}{TW \sum_{l=0}^{k} \sum_{i=1}^{M+1} \left(\phi_l^{(i)} + \tau \sum_{j \in \mathcal{N}_i} p_l^{(i,j)} \right)}. \tag{23}$$

In addition to this, we compare the performance of the network in terms of the total data arrived at the sink node, and/or the total data transmitted across the network.

In the comparison of the solution of the offline original non-convex problem (15) with the solution of the offline approximated convex problem (16) using the global solver SCIP, we consider simulation over 50 time-slots due to the run-time complexity and heavy memory requirement of the global solver. The comparison is carried out in terms of the energy efficiency and the data transmitted across the network, with zero processing and non-zero processing costs. As shown in Figure 3, the energy efficiency of the original problem is higher than that of the approximated convex problem. However, we observe that both solutions exhibit similar trends of the energy efficiency as a function of time-slot k. The energy efficiency obtained by the SCIP solver, peaks at the beginning and then smooths out as time progresses. Similarly, the data transmitted across the network of both problems exhibit similar trend as a function of time-slot k, with a slight increase for the approximated problem.

The average energy efficiency of OMA and NOMA based EH-WSN is shown in Figure 4 for the offline, MPC and DMPC resource allocation algorithms computed at the sink node, and across the network. The simulations are conducted over 100 time-slots, and averaged over 100 runs. The receding horizon for MPC and DMPC based resource allocation techniques is chosen as $N = 5$ time-slots. The results are shown for

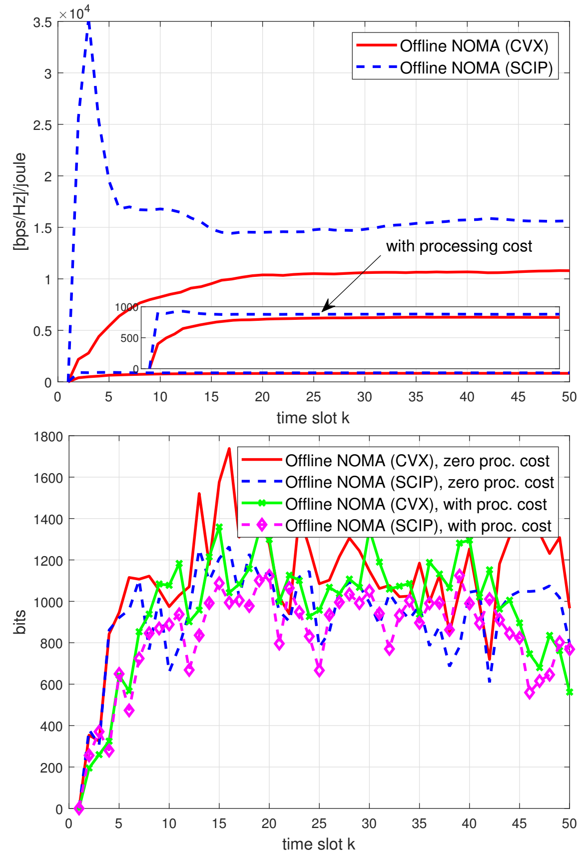

Fig. 3. Top: energy efficiency across the network EE_k^{global}. Bottom: data transmitted across the network.

zero and non-zero processing costs. As clear from the figure, the average energy efficiency of NOMA outperforms the average energy efficiency of OMA in all resource allocation techniques, when zero-processing cost is considered. For non-zero processing cost, the average energy efficiency of OMA slightly outperforms that of NOMA. As expected, the offline based resource allocation outperforms MPC and DMPC based resource allocation for OMA and NOMA techniques. Nonetheless, MPC and DMPC resource allocation follows the same trend as of that of the offline. The performance gap is due to the fact that offline relies on non-causal information of the EH-WSN.

To give a complete picture, we examine the average transmitted data reached the sink node, and the average transmitted data across the network as shown in Figure 5. It is clear from the figure that the processing cost has no effect on the average amount of data transmitted across the network or that arrived at the sink. The average amount of data transmitted across the network or that arrived at the sink node, constantly larger for NOMA compared to OMA. We observe identical performance for NOMA offline and NOMA MPC. The performance of NOMA DMPC is slightly below that of NOMA offline and MPC, and still outperforms OMA DMPC.

The empirical cumulative distribution function (CDF) of the transmitted data across the network and the empirical CDF of the transmitted power are shown in Figure 6. The empirical CDFs are only shown for zero processing cost. For non-zero

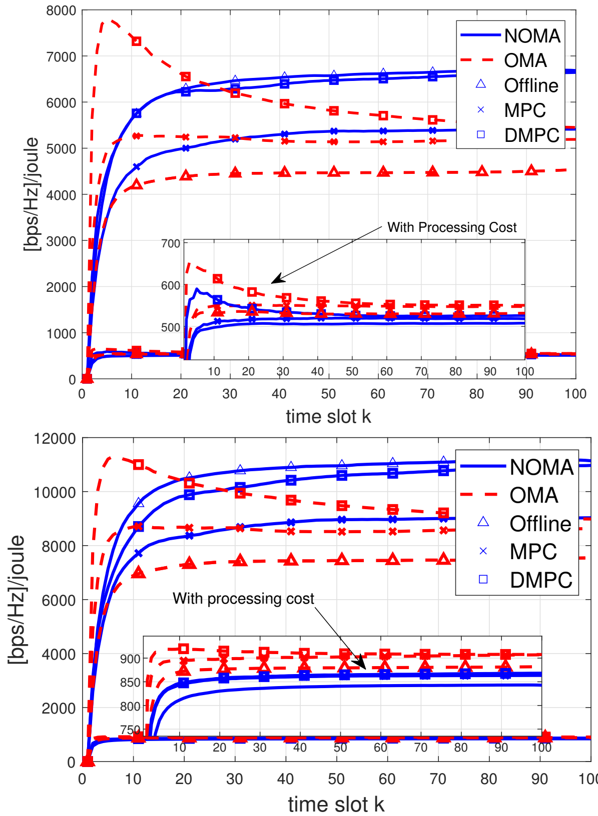

Fig. 4. Top: the average energy efficiency computed at the sink EE_k^{sink}. Bottom: the average energy efficiency across the network EE_k^{global}.

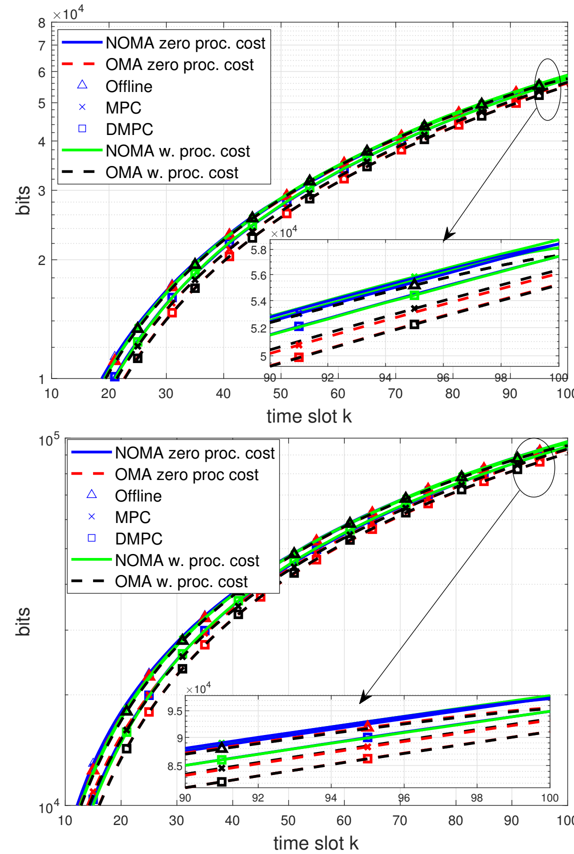

Fig. 5. Top: the average data received at the sink. Bottom: the average data transmitted across the network.

processing cost we observe exactly the same empirical CDF for the transmitted data and for the transmission power. As clear from this figure, the transmission power empirical CDF of the resource allocation techniques are almost similar for NOMA/OMA. At high probability NOMA, is more conservative in using power than that of OMA. For the transmitted data, the CDF of the offline NOMA and OMA techniques are almost similar. NOMA MPC and DMPC are more conservative in data transmission compared to OMA and/or offline NOMA at high probability. This explains the small average energy efficiency with processing cost compared to zero-processing cost.

V. Conclusion

In this paper, we considered optimal power management for multi-hop EH-WSN using NOMA. The power control problem aiming to transmit the data of all sensor nodes using minimum energy was approximated as a convex finite horizon dynamic programming problem. We considered the non-causal offline and the causal online problems. The online optimal power control was obtained based on MPC framework. A distributed MPC was proposed to solve smaller local MPC sub-problems that can be solved simultaneously at a much lower computational complexity. The performance of the proposed algorithms were measured in terms of the average energy efficiency and average data transmitted under zero-processing and non-zero-processing costs assumptions. The processing cost was modeled as an affine function in the transmitted and decoded data. The average energy efficiency is significantly affected by the processing cost, while the average data transmitted is not. The average data transmitted (throughput) of NOMA is generally higher than that of OMA. From the empirical CDF of the transmission power, NOMA is more conservative in using the available power compared to OMA. This motivates further investigations of resource management in dynamic systems using NOMA. Considering parametric MPC/DMPC model is also an interesting direction to reduce the computational complexity of the solution using a look up table and avoiding to solve an optimization problem at each time-slot.

References

[1] X. Zhang, H. Qi, X. Zhang, and L. Han, "Energy-efficient resource allocation and data transmission of cell-free internet of things," *IEEE Internet of Things Journal*, pp. 1–1, 2020.

[2] "Number of internet of things (IoT) connected devices worldwide in 2018, 2025 and 2030 (in billions) [graph]," https://www.statista.com/statistics/802690/worldwide-connected-devices-by-access-technology/, strategy Analytics, In Statista. May 16, 2019.

[3] C. K. Ho and R. Zhang, "Optimal energy allocation for wireless communications with energy harvesting constraints," *IEEE Trans. Signal Process.*, vol. 60, no. 9, pp. 4808–4818, Sep. 2012.

[4] C. Mahapatra, Z. Sheng, P. Kamalinejad, V. C. M. Leung, and S. Mirabbasi, "Optimal power control in green wireless sensor networks with wireless energy harvesting, wake-up radio and transmission control," *IEEE Access*, vol. 5, pp. 501–518, 2017.

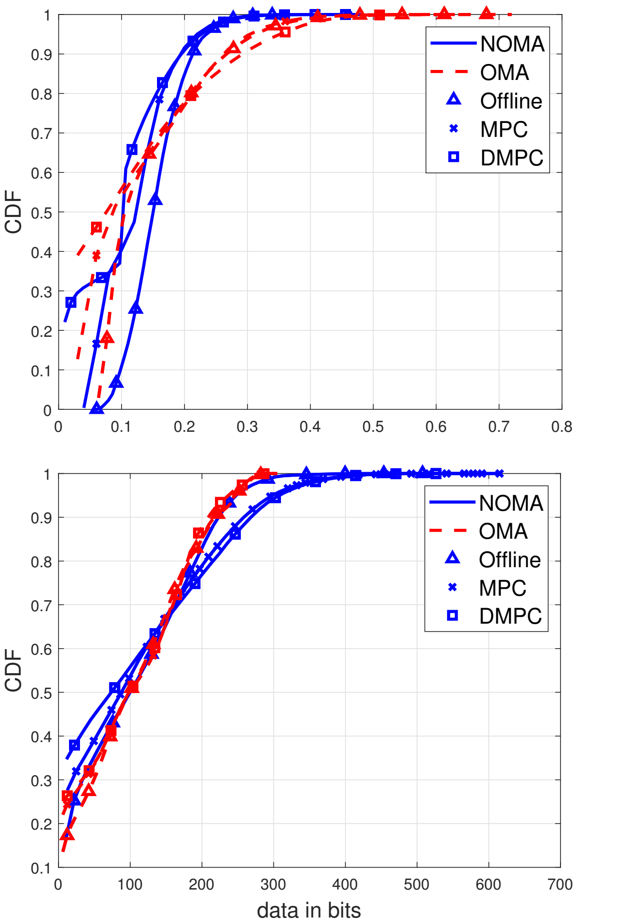

Fig. 6. Top: empirical CDF for the transmission power. Bottom: empirical CDF for the transmitted data.

[5] D. Altinel and G. Karabulut Kurt, "Modeling of multiple energy sources for hybrid energy harvesting IoT systems," *IEEE Internet of Things Journal*, vol. 6, no. 6, pp. 10 846–10 854, 2019.

[6] Q. Wu, G. Y. Li, W. Chen, D. W. K. Ng, and R. Schober, "An overview of sustainable green 5G networks," *IEEE Wireless Commun. Mag.*, vol. 24, no. 4, pp. 72–80, Aug. 2017.

[7] S. M. R. Islam, N. Avazov, O. A. Dobre, and K. Kwak, "Power-domain non-orthogonal multiple access (NOMA) in 5G systems: Potentials and challenges," *IEEE Communications Surveys Tutorials*, vol. 19, no. 2, pp. 721–742, 2017.

[8] J. Zhu, J. Wang, Y. Huang, S. He, X. You, and L. Yang, "On optimal power allocation for downlink non-orthogonal multiple access systems," *IEEE Journal on Selected Areas in Communications*, vol. 35, no. 12, pp. 2744–2757, 2017.

[9] F. Borrelli, A. Bemporad, and M. Morari, *Predictive Control for linear and hybrid systems*. UK: Cambridge University Press, 2017.

[10] E. Stai and S. Papavassiliou, "Receding horizon control for an online cross-layer design of wireless networks over time-varying stochastic channels," *IEEE Trans. Wireless Commun.*, vol. 16, no. 6, pp. 3814–3826, Jun. 2017.

[11] D. Gu, "A differential game approach to formation control," *IEEE Trans. Control Syst. Technol.*, vol. 16, no. 1, pp. 85–93, Jan. 2008.

[12] O. Mokrenko, M. I. Vergara-Gallego, W. Lombardi, S. Lesecq, D. Puschini, and C. Albea, "Design and implementation of a predictive control strategy for power management of a wireless sensor network," in *Proc. European Control Conference, (ECC)*, 2015, pp. 2303–2308.

[13] H. Al-Tous and I. Barhumi, "Differential game for resource allocation in energy harvesting wireless sensor networks," *IEEE Transactions on Green Communications and Networking*, vol. 4, no. 4, pp. 1165–1173, 2020.

[14] H. Al-Tous and I. Barhumi, "MPC for online power control in energy harvesting sensor networks," in *Proc. of the IEEE 87th Vehicular Technology Conference, (VTC-Spring)*, June 2018, pp. 1–5.

[15] Z. Yang, W. Xu, Y. Pan, C. Pan, and M. Chen, "Energy efficient resource allocation in machine-to-machine communications with multiple access and energy harvesting for IoT," *IEEE Internet of Things Journal*, vol. 5, no. 1, pp. 229–245, 2018.

[16] D. Jiao, P. Yang, L. Fu, L. Ke, and K. Tang, "Optimal energy-delay scheduling for energy-harvesting wsns with interference channel via negatively correlated search," *IEEE Internet of Things Journal*, vol. 7, no. 3, pp. 1690–1703, 2020.

[17] D. Jiao, L. Ke, S. Liu, and F. T. Chan, "Optimal energy-delay in energy harvesting wireless sensor networks with interference channels," *Sensors*, vol. 19, no. 4, 2019. [Online]. Available: https://www.mdpi.com/1424-8220/19/4/785

[18] Z. Yang, Z. Ding, P. Fan, and N. Al-Dhahir, "A general power allocation scheme to guarantee quality of service in downlink and uplink NOMA systems," *IEEE Transactions on Wireless Communications*, vol. 15, no. 11, pp. 7244–7257, 2016.

[19] Y. Zhang, H.-M. Wang, T.-X. Zheng, and Q. Yang, "Energy-efficient transmission design in non-orthogonal multiple access," *IEEE Transactions on Vehicular Technology*, vol. 66, no. 3, pp. 2852–2857, 2017.

[20] G. Franze, A. Casavola, D. Famularo, and W. Lucia, "Distributed receding horizon control of constrained networked leader-follower formations subject to packet dropouts," *IEEE Trans. Control Syst. Technol.*, vol. PP, no. 99, pp. 1–12, 2017.

[21] B. Krishnamachari, *Networking Wireless Sensors*. UK: Cambridge University Press, 2005.

[22] A. Arafa and S. Ulukus, "Optimal policies for wireless networks with energy harvesting transmitters and receivers: Effects of decoding costs," *IEEE J. Sel. Areas Commun.*, vol. 33, no. 12, pp. 2611–2625, Dec. 2015.

[23] G. Gamrath and et al., "The SCIP Optimization Suite 7.0," Zuse Institute Berlin, ZIB-Report 20-10, March 2020. [Online]. Available: http://nbn-resolving.de/urn:nbn:de:0297-zib-78023

[24] S. Boyd and L. Vandenberghe, *Convex Optimization*. Cambridge University Press, 2004.

[25] M. Kamel, K. Alexis, M. Achtelik, and R. Siegwart, "Fast nonlinear model predictive control for multicopter attitude tracking on SO(3)," in *Proc. of the IEEE Conference on Control Applications, (CCA)*, Sep. 2015, pp. 1160–1166.

[26] A. Alessio, D. Barcelli, and A. Bemporad, "Decentralized model predictive control of dynamically coupled linear systems," *Journal of Process Control*, vol. 21, no. 5, pp. 705–714, 2011.

[27] M. Farina and R. Scattolini, "Distributed predictive control: A non-cooperative algorithm with neighbor-to-neighbor communication for linear systems," *Automatica*, vol. 48, no. 6, pp. 1088–1096, 2012.

[28] P. Blasco, D. Gunduz, and M. Dohler, "A learning theoretic approach to energy harvesting communication system optimization," *IEEE Trans. Wireless Commun.*, vol. 12, no. 4, pp. 1872–1882, Apr. 2013.

[29] M. Grant and S. Boyd, "CVX: Matlab software for disciplined convex programming, version 2.1," http://cvxr.com/cvx, Mar. 2014.

Imad Barhumi (M'2005, SM'2013) received the B.Sc. degree in electrical engineering from Birzeit University, Birzeit, Palestine, in 1996, the M.Sc. degree in telecommunications from the University of Jordan, Amman, Jordan, in 1999, and the Ph.D. degree in electrical engineering from the Katholieke Universiteit Leuven (KUL), Leuven, Belgium, in 2005. From 1999 to 2000, he was with the Department of Electrical Engineering, Birzeit University, as a Lecturer. After his Ph.D. graduation, he was a Postdoctoral Research Fellow for one year with the Department of Electrical Engineering, KUL. He is currently an Associate Professor with the Department of Electrical Engineering, United Arab Emirates University, Al Ain, United Arab Emirates. His research interests include signal processing for mobile and wireless communications, cooperative communications, resource allocation and management in wireless communications and networking, game theory and compressive sensing.

Hanan Al-Tous (M'2000, SM' 2017) received the B.Sc. degree in Electrical Engineering in 1998 and the M.Sc. in Communication Engineering in 2000 from the University of Jordan, Amman, Jordan, and the Ph.D. degree in electrical engineering in 2014 from United Arab Emirates University, Al Ain, United Arab Emirates She worked as a lecturer with the Electrical Engineering Department, Al-Ahliyya Amman University, Amman, Jordan from 2000-2010. She worked as a postdoc at the United Arab Emirates University, Al Ain, United Arab Emirates from 2014-2018. She is currently a research fellow at Aalto University, Finland. Her research interests include cooperative communications, energy harvested sensor networks, resource allocation for wireless communications, game theory, compressive sensing and machine learning.